

Pedestrian Tracking and Navigation Using Neural Networks and Fuzzy Logic

Charles Toth, Dorota A. Grejner-Brzezinska, Shahram Moafipoor
Center for Mapping, The Ohio State University
1216 Kinnear Road
Columbus, OH 43212 USA

Abstract –The main goal of the research presented here is to develop theoretical foundations and implementation algorithms, which integrate GPS, micro-electro-mechanical inertial measurement unit (MEMS IMU), digital barometer, electronic compass, and human pedometry to provide navigation and tracking of military and rescue ground personnel. This paper discusses the design, implementation and the initial performance analyses of the personal navigator prototype¹, with a special emphasis on dead-reckoning (DR) navigation supported by the human locomotion model. To facilitate this functionality, the adaptive knowledge system, based on the Artificial Neural Networks (ANN) and Fuzzy Logic, is trained during the GPS signal reception and used to maintain navigation under GPS-denied conditions. The human locomotion parameters, step frequency (SF) and step length (SL) are estimated during the system calibration period, then the predicted SL, together with the heading information from the compass and gyro, support DR navigation. The current target accuracy of the system is 3-5 m CEP (circular error probable) 50%.

Keywords – Artificial Neural Network, Fuzzy Logic, Kalman-filtering, Personal navigation.

I. INTRODUCTION

Personal navigation is concerned with providing position information in real-time to support navigation and tracking of military and rescue ground personnel. Navigation systems that offer position information can be categorized as: (1) satellite-based Global Navigation Satellite System (GNSS), (2) local or regional RF network-based systems, and (3) multi-sensor systems. While the GNSS-based positioning generally supports outdoor applications, the network-based category utilizes the existing communication network infrastructure, such as wireless local area network (WLAN), Bluetooth or radio frequency ID (RFID), where the user

location (indoor or outdoor) is determined based on the received signal strength, angle of arrival, time of arrival or the difference in time of arrival. In addition to GNSS/RF navigation, multi-sensor systems typically incorporate additional sensors or sensor networks such as inertial measurement units (IMUs), magnetometers, laser scanners, infrared sensors, optical imagers, etc. to provide absolute or relative position information. Recent technological developments in positioning and tracking sensors, including the Global Positioning System (GPS) modernization program and advances in high-sensitivity receiver technology, capable of supporting navigation indoors and in confined environments [14], well-established MEMS accelerometer technology, and steadily improving MEMS gyro technology, miniaturized magnetometers and digital barometer/altimeter technology, as well as the availability of other RF signals capable of supporting navigation offer a potential to develop multi-sensor, portable systems for personal tracking and navigation for outdoor and indoor environments with one to a few meters accuracy.

Personal navigation has been of research interest for a number of years; two primary approaches are (1) multi-sensor sensor integration, e.g., [2, 5, 17, 13], and (2) pedometry, e.g., [3, 4]. Both approaches have their advantages and disadvantages; thus, the next logical step is to integrate these two approaches to form an intelligent navigation system, where the term *intelligent navigation* represents the transition from the conventional GPS/IMU-based system to multi-sensor systems that increasingly rely on integrating adaptive knowledge systems (AKS) based on, for example, artificial neural networks (ANN), fuzzy logic (FL), etc., to accommodate human locomotion modeling to support navigation in dead reckoning (DR) mode. Furthermore, the scope of applications of navigation technologies is expanding from the typical open sky environment (where GNSS is the primary navigation means) to indoor and confined environments, such as urban and underground settings. In this evolution, a variety of new sensors, such as electronic

¹ This research is supported by a 2004 National Geospatial-Intelligence Agency NURI project

compasses, barometers, motion sensors, RF signals of opportunity, GIS/CAD (Geographic Information Systems/Computer Aided Design) map data, etc. are employed. Consequently, the traditional Extended Kalman Filter (EKF) approach to multi-sensory data integration may no longer be able to properly handle the often non-Gaussian and nonlinear measurement models and more complex dynamic models. As a result, nonlinear Bayesian Filters, such as Unscented Kalman Filter (UKF) and Particle Filter (PF) have been recently introduced to navigation applications, see, for example, [10, 22, 15, 18, 9], and nontraditional approaches to sensor integration and modeling, such as Artificial Neural Networks (ANN) [11, 23, 6, 7], and fuzzy logic, e.g., [20, 1] are considered for navigation algorithms. In the pedestrian navigation system proposed by [21], a knowledge-based component is used for outlier detection in the observation data and the quality analysis and calibration of the multi-sensor system. In the increasingly more complex environments, data and dynamic models, ANN and fuzzy logic form a basis for adaptive knowledge systems, needed to handle the intricacy of a wide range of data entities as well as their rapidly changing availability in different environments. The knowledge systems can work in a variety of ways, such as individual agents monitoring input signal conditions and controlling the EKF (or, alternatively, UKF or PA) with adaptive error models or even replacing the EKF with an alternative solution (such as Fuzzy Kalman Filter).

This paper presents a concept design, prototype implementation and performance analysis of a personal navigator based on multi-sensor integration, augmented by the human locomotion model that supports navigation during GPS gaps. The navigation accuracy requirement is considered at 3-5 m CEP (circular error probable) 50% level. The performance analysis presented here is focused on (1) human dynamics (locomotion) modeling using the adaptive knowledge system, and (2) dead reckoning navigation using the calibrated human dynamics model (step length (SL)). The training process of the knowledge system during the GPS signal availability is discussed, and the accuracy of the SL recovery is presented; subsequently, the DR navigation accuracy is demonstrated using the trained human dynamics model. The accuracy of the DR trajectory is determined based on the reference GPS/IMU trajectory. Finally, the summary, conclusions and future research are presented.

II. PROTOTYPE SYSTEM DESIGN

The conceptual design of the current system is depicted in Fig. 1. The primary four sensors, GPS, IMU, barometer, and compass are integrated in a tightly coupled Extended Kalman Filter (EKF), where carrier phase and/or pseudorange data are used to obtain a full navigation solution, as well as calibrated IMU errors. The barometer and compass are introduced to aid height and heading estimation, respectively, when GPS signals are blocked. In addition, heel and toe contact switches are also used to record the pedestrian motion, providing a direct observation of SF. These sensors are continuously

calibrated during GPS signal availability, see blue lines in Fig 1, while in DR mode, there is no sensor calibration, blue lines are inactive, and the positions estimates are provided based on sensor data and AKS, red lines.

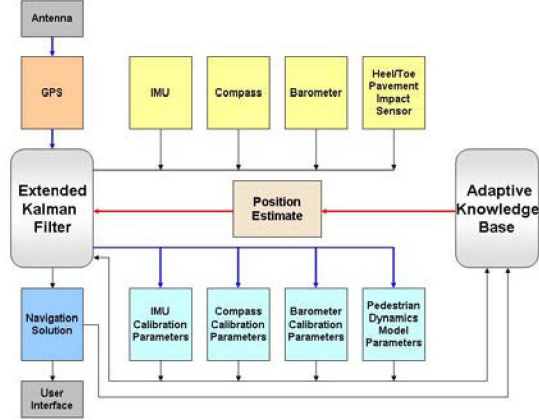


Fig. 1. Personal navigator: system architecture; training mode (blue) and dead reckoning mode (red)

The EKF has been the workhorse of GPS/IMU-based navigation systems for a long time. Under normal conditions, with good GPS signal availability, the EKF provides excellent navigation solution, depending on the quality of the IMU sensors used. Note the compass may contribute to calibrating and aiding the IMU sensors. For GPS-denied situations, when no other aiding is available the IMU errors will get no fixes and thus the solution drifts away. In particular, this is the case when medium- or low-grade IMU's are used. In our implementation, the state vector \vec{x} includes 3 position errors, 3 velocity errors, and 3 attitude component errors, 3 accelerometer biases and 3 scale factors, 3 gyro biases and 3 scale factors, as well as 2 barometer and 2 (4) compass (magnetometer) errors, as listed in Table 1.

TABLE I.
STOCHASTIC ERROR MODELS FOR MULTI-SENSOR ERROR SOURCES

Sensor	Error Source	Stochastic Error Model
Accelerometer	Bias	Random walk
	Scale factor	Random constant
Gyroscope	Bias	Random walk
	Scale factor	Random constant
Barometer	Bias	Random constant
	Scale factor	Random walk
Digital compass	Bias	Random constant
	Scale factor	Random walk

$$\begin{bmatrix} \dot{x}_{\text{Nav}} \\ \dot{x}_f \\ \dot{x}_\omega \\ \dot{x}_B \\ \dot{x}_C \end{bmatrix} = \begin{bmatrix} F_{11} & F_{12} & F_{13} \\ & F_{22} & \\ & & F_{33} \\ & & & F_{44} \\ & & & & F_{55} \end{bmatrix} \begin{bmatrix} x_{\text{Nav}} \\ x_f \\ x_\omega \\ x_B \\ x_C \end{bmatrix} + \begin{bmatrix} u_{\text{Nav}} \\ u_f \\ u_\omega \\ u_B \\ u_C \end{bmatrix} \quad (1)$$

where:

$$F_{11} = \begin{bmatrix} 0 & -\dot{\lambda}sL & \dot{\lambda} & 1 & 0 & 0 & 0 & 0 \\ \dot{\lambda}sL & 0 & \dot{\lambda}cL & 0 & 1 & 0 & 0 & 0 \\ -\dot{\lambda} & -\dot{\lambda}cL & 0 & 0 & 0 & 1 & 0 & 0 \\ -\frac{g}{R_e} & 0 & 0 & 0 & -(2\omega_b + \dot{\lambda})sL & \dot{\lambda} & 0 & -f_D \\ 0 & -\frac{g}{R_e} & 0 & (2\omega_b + \dot{\lambda})sL & 0 & (2\omega_b + \dot{\lambda})cL & f_D & 0 \\ 0 & 0 & \frac{2g}{R_e} & -\dot{L} & -(2\omega_b + \dot{\lambda})cL & 0 & -f_E & f_N \\ 0 & 0 & 0 & 0 & 0 & 0 & -(\omega_b + \dot{\lambda})sL & \dot{L} \\ 0 & 0 & 0 & 0 & 0 & (\omega_b + \dot{\lambda})sL & 0 & -(\omega_b + \dot{\lambda})sL \\ 0 & 0 & 0 & 0 & 0 & -\dot{L} & (\omega_b + \dot{\lambda})sL & 0 \end{bmatrix} \quad (2)$$

where

($sL = \sin(L)$, $cL = \cos(L)$)

$$F_{12} = \begin{bmatrix} 0(3 \times 3) & 0(3 \times 3) \\ C_b^n & C_b^n \begin{bmatrix} f_x & 0 & 0 \\ 0 & f_y & 0 \\ 0 & 0 & f_z \end{bmatrix} \\ 0(3 \times 3) & 0(3 \times 3) \end{bmatrix} \quad (3)$$

$$F_{13} = \begin{bmatrix} 0(6 \times 3) & 0(6 \times 3) \\ -C_b^n & -C_b^n \begin{bmatrix} \omega_x & 0 & 0 \\ 0 & \omega_y & 0 \\ 0 & 0 & \omega_z \end{bmatrix} \end{bmatrix} \quad (4)$$

$$\begin{bmatrix} F_{22} & & \\ & F_{33} & \\ & & F_{44} \\ & & & F_{55} \end{bmatrix} = \begin{bmatrix} 0_{6 \times 6} & & \\ & 0_{6 \times 6} & \\ & & 0_{2 \times 2} \\ & & & 0_{4 \times 4} \end{bmatrix} \quad (5)$$

The state transition matrix F is shown in equations 1-5, where u_{Nav} , u_f , $u_\omega u_B$ and u_C are the zero-mean white noise vector processes corresponding to navigation, accelerometer, gyroscope, barometer and compass (magnetometer) states, respectively; the components of vector u corresponding to variables modeled as random constant (see, Table 1) are zero.

In the equations above, C_b^n is the direction cosine matrix from body-fixed frame (b -frame) to navigation frame (n -frame), ω_i is the Earth's rotation rate, L is the geodetic latitude, λ is the geodetic longitude, g is the gravity constant, (f_x, f_y, f_z) is the accelerometer sensed specific force vector defined in the b -frame, (f_N, f_E, f_D) is the same specific force vector coordinatized in the b -frame, $(\omega_x, \omega_y, \omega_z)$ is the gyro-sensed rotation rate vector, and R_e is the Earth radius [9]. The remaining elements of matrix F in equation (1) are zero.

The sensor suite of the current prototype includes a dual frequency Novatel OEM4 GPS receiver with TRM22020.00+GP antenna, Crossbow MEMS IMU 400CC, Honeywell tactical grade HG1700 IMU, impact foot switches used for timing the operator step events, PTB220A barometer (500–1100hPa pressure range, -40–140F temperature range, 0.5–10Hz update rate, 0.1–3s output averaging time, and 1.5 m height accuracy (1σ)), KVH Azimuth digital compass, (25° gimbal rate, 20 Hz read-out rate, 1° heading accuracy), and a three-axis Honeywell HMR3000 magnetometer with an integrated pitch-roll sensor (20 Hz read-out rate, 1° (level), and 2° (tilt) heading accuracy (1σ)). The HG1700 IMU and the HMR3000 magnetometer were added later to replace the

sensors that didn't meet accuracy specifications. The GPS carrier phase and pseudorange measurements in the double difference (DD) mode, barometric height, compass (magnetometer) heading, and the INS-derived position and attitude information are integrated together in the tightly coupled EKF with 27 states (see, Equation 1 and Table 1). The prototype is based on a backpack sensor configuration, as shown in Fig. 2.

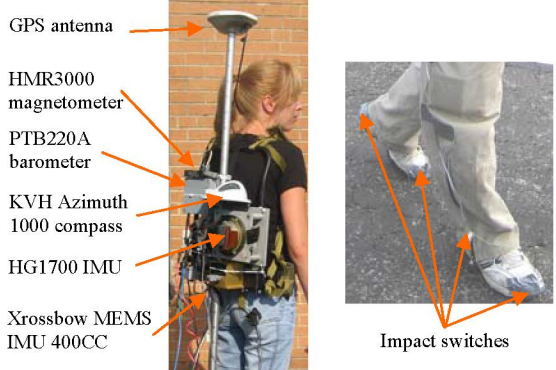


Fig. 2. Backpack prototype system; data recording and processing system, including OEM4 GPS receiver, is not shown.

III. ADAPTIVE KNOWLEDGE SYSTEM

The main objective of the AKS module in our design is to model the human locomotion in training mode and then provide estimates for SL in DR mode; the current implementation incorporates ANN and FL components. The navigation solution is used to train the adaptive knowledge system that (1) stores the information about the human locomotion model (SL), and subsequently uses it to navigate in dead-reckoning mode during the GPS signal blockage (see, Grejner-Brzezinska, 2006a, b), or (2) uses an ANN- or FL-based approach of AKS training, which will then work in the prediction mode to evaluate SL based on the training data (or acquired knowledge) and input parameters that are provided in DR mode.

A. Parameter Preprocessing

Based on the prototype sensor configuration, six parameters that contain the information about the step length (SL), such as step frequency (SF), peak-to-peak mean acceleration ($|a|$), peak-to-peak variation in acceleration ($\text{Var}|a|$), terrain slope, change in barometric height during a single gait cycle (Δh_{baro}), and operator's height were selected. To remove correlation from the input data, Principal Component Analysis (PCA) was performed on a larger training set; prior PCA, the mean was removed and the data was normalized to a uniform range. Results indicated medium parameter correlation and consequently reducing the parameter space to three components, based on the three largest eigenvalues, achieved a near identical performance with respect to using all the six parameters, as shown later. For details on the PCA-based data preprocessing see [7].

B. ANN-based Adaptive Knowledge System

A single-layer artificial neural network with Radial Basis Function (RBF) was selected as an alternative to a multilayer perceptron (MLP) since simpler to train, even though it typically needs more neurons than MLP [16]. In Fig. 3, n , the number of RBF functions, ranges between 30 and 40 in a single hidden layer, and one output parameter, SL, is provided; note that all the input parameters are shown. The ANN learning rate was empirically selected as 0.05, and the total number of iterations is normally around 500.

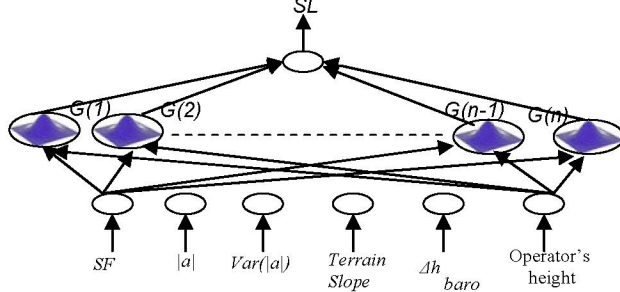


Fig. 3. Conceptual design of the RBF-based ANN.

C. FL-based Adaptive Knowledge System

The newest update to the system design is the addition of the fuzzy-logic-based component of AKS to support SL modeling and facilitate other types of external information, such as indoor or outdoor map information/constraints that can be introduced to AKS in the form of membership functions developed during the training process. By incorporating fuzzy logic [19, 12] to our AKS, better process control and more reliable SL prediction are expected. This approach should also facilitate an easy addition of constraints, such as, for example, a hallway layout for indoor navigation, or digital map information, which may be difficult to handle in an EKF environment. In the current prototype implementation, 58 fuzzy rules are formulated by fuzzy definition of individual behaviors of the variables provided by various sensors (accelerometers, compass, barometer, gyroscopes, hallway layout of a building for indoor navigation, etc.), and their diverse contributions to the SL model. In essence, training data are collected for each operator separately, and functions, such as, SF, rate of SF, terrain slope, operator's locomotion pattern (e.g., standing, walking, jogging, sprinting, climbing, etc.), etc., as a function of sensor outputs are analyzed to form the fuzzy rules that are subsequently used in the actual DR navigation mode.

IV. EXPERIMENTAL RESULTS

The first test dataset was collected in September 2005 using all sensors listed earlier, and used for performance assessment of the personal navigator, with the emphasis on the dead reckoning mode. Two operators A and B walked a loop with ~ 355 m circumference three times; each loop was approximately 130-135 full gait cycles; SL results are shown

in Table II. The reference trajectory was generated using GPS/IMU data (double-difference carrier phase plus HG1700 measurements), and DR mode was artificially enforced by introducing GPS gaps. Various cases of SL calibration are presented and compared. Subsequently, the estimated SL is used for trajectory prediction in DR during GPS outages. In all cases the trajectory is estimated using the respective SL and a reference heading (from GPS/IMU solution) to test the impact of SL modeling on trajectory reconstruction.

TABLE II.
SL: NUMERICAL RESULTS; AVERAGE VALUES PER LOOPS

Operator/Loop	Operator A		Operator B	
	Mean [m]	Std [m]	Mean [m]	Std [m]
Loop 1	0.61	0.05	0.67	0.06
Loop 2	0.63	0.04	0.64	0.09
Loop 3	0.72	0.10	0.72	0.09

A. Using Fixed-Length SL on Flat Terrain

Fig. 4 illustrates the example comparison of the DR trajectory with the reference trajectory for operator A, where reference heading and the average SL=75 cm from loop 3 were used to generate the DR trajectory. Fig. 5 depicts the loop 3 trajectory reconstruction, where variable SL was used for different geometric parts of the trajectory (SL=95 for both straight portions, and SL=85 cm for both curved portions of the trajectory), clearly demonstrating the effect of adapting SL to better fit the overall trajectory; note, that SL=95 cm was obtained by rescaling the SL=72 cm to 1 second sampling rate. The results clearly indicate a significant improvement when varying SL was used for different portions of the trajectory, as compared to using an average step length to reconstruct the entire trajectory. In numerical terms, CEP 50% was 4.7 m and 1.1 m, respectively, meeting the project specifications of 3-5 m for all cases. Note that these statistics account only for the error in SL (no heading error included).

B. ANN-based SL Modeling on Flat Terrain

To verify the performance of the AKS-based SL prediction in DR navigation mode, the ANN was used to predict the operator's trajectory for the same loop. Fig. 6 illustrates the comparison of the reference trajectory (blue), the trajectory generated using the SL predicted by the ANN, where the input parameters were not PCA-transformed (green), and where the input parameters were PCA-transformed (red). The statistics of the DR trajectories' fit to the reference trajectory are presented in Table III. The end misclosure of the resulting trajectory was 1.16m with the mean (std) and maximum departures from the reference trajectory equal to 0.33m (0.32m) and 1.07m, respectively. Clearly, the PCA-based input parameter pre-processing improves the ANN performance. Note that both CEP's (50% and 95%) meet the performance specifications of 3-5m. Similar to earlier results, these statistics account only for the error in SL.

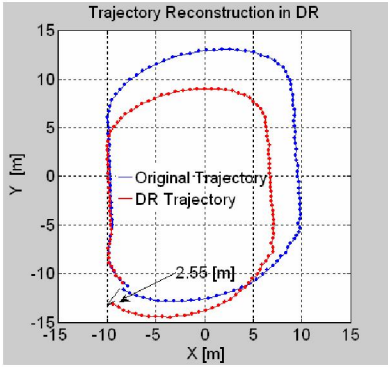


Fig. 4. DR trajectory reconstruction for loop 3, operator A using average SL=75 cm.

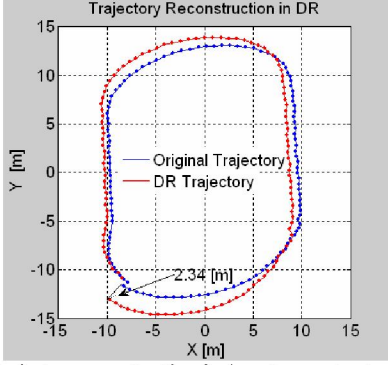


Fig. 5. DR trajectory reconstruction for loop 3, operator A using varying step length as a function of trajectory dynamics/geometry; SL = 95 for the straight portions and SL = 85 cm for the curved portions.

TABLE III.

STATISTICAL FIT TO REFERENCE TRAJECTORY OF DR TRAJECTORY GENERATED WITH SL PREDICTED BY ANN WITH AND WITHOUT PCA TRANSFORMATION (NO PARAMETER SPACE REDUCTION)

Solution type	Mean [m]	Std [m]	Max Difference [m]	End Misclosure [m]	CEP 50% [m]	CEP 95% [m]
DR no PCA	1.7	1.4	4.7	2.3	1.3	4.4
DR with PCA	0.33	0.32	1.07	1.16	0.3	1.0

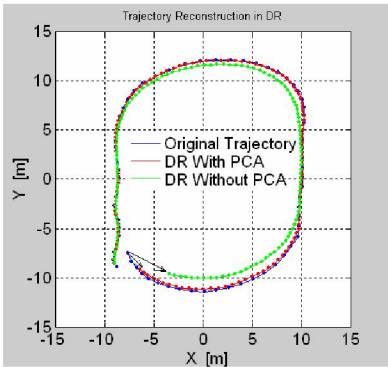


Fig. 6. Comparison of the reference trajectory (blue), trajectory generated using ANN-predicted SL where the input parameters were not PCA-transformed (green), and where the input parameters were PCA-transformed (red).

C. Comparing ANN- and FZ-based SL Modeling

To analyze the performance of the ANN- and FZ-based SL prediction in DR navigation mode and to consider sloping terrain, a second test was performed in April 2006 that included the OSU Campus loop and hilly area nearby. Fig. 7 shows the trajectories created by the ANN and FZ SL-prediction for the flat loop area (with PCA preprocessing).

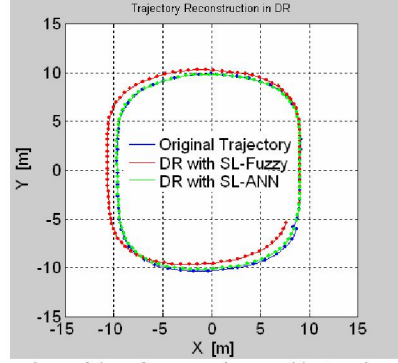


Fig. 7. Comparison of the reference trajectory (blue), trajectory generated using ANN-predicted SL (green), trajectory generated using FL-predicted SL (red) on a flat area.

Fig. 8 shows the trajectories created by the ANN and FZ SL-prediction for a moderately sloping area (about 3-5%).

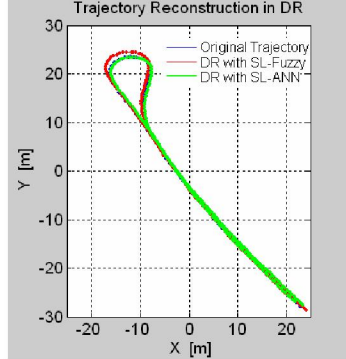


Fig. 8. Comparison of the reference trajectory (blue), trajectory generated using ANN-predicted SL (green), trajectory generated using FL-predicted SL (red) on a sloping area.

Statistical results, shown in Table IV, indicate that the accuracy of the reconstructed trajectories is comparable for both methods; note the results of an additional test with slightly steeper terrain were also included (test 3). Clearly, the ANN-based solution provides a somewhat smaller end misclosure, mean and std, but the fuzzy-logic-based solution's flexibility and potential for process control support is definitely worth pursuing. Further development of relevant membership functions to assure better process control, more flexibility and potential for process control support and more reliable SL prediction is currently underway. This mechanism will also allow for an easy addition of constraints, for example, hallway layout for indoor navigation, and for implementation of an adaptive algorithm for covariance propagation in EKF.

TABLE IV.

STATISTICAL FIT TO REFERENCE TRAJECTORY OF TRAJECTORIES GENERATED USING SL PREDICTED WITH ANN AND FL FOR THREE DIFFERENT DATA SETS

Test dataset	SL modeling	Mean [m]	Std [m]	Max Difference [m]	End Misclosure [m]	CEP 50% [m]	CEP 95% [m]
1	FL	1.04	0.53	1.66	0.54	1.22	1.62
	ANN	0.21	0.14	0.52	0.26	0.19	0.49
2	FL	0.91	0.47	1.63	0.87	1.07	1.57
	ANN	0.19	0.16	0.58	0.22	0.11	0.51
3	FL	0.91	0.47	1.63	0.87	1.07	1.57
	ANN	0.19	0.16	0.58	0.22	0.11	0.51

V. CONCLUSIONS

The prototype of human locomotion modeling (step length, SL) using ANN- and FL-based AKS to support personal navigation in DR mode during GPS signal blockage/jamming was presented. Sample training and testing data were collected on a level surface in three circular paths and on sloping terrain by different operators. The focus of the study presented here was on assessing and improving the efficiency of ANN/FL training and the reliability of ANN/FL prediction of SL as a function of input data selection and space reduction. During the tests, six parameters were recorded and preprocessed, and then used as input to the ANN/FL system in various combinations in both training and testing modes. The results showed that CEP 50% < 5m in positioning performance could be consistently achieved for the few hundred meter long trajectories with mild to fair slopes and moderate operator maneuvering, using the ANN/FL step length modeling (note that reference heading was used in all tests presented here). In addition, it was demonstrated that a PCA transformation efficiently removes the correlation among the input parameters, and can also reduce the input data dimensionality to optimize the training process, and subsequently, decrease the complexity/size of the ANN. Thus, the optimum combination of the PCA-transformed parameters in reduced input parameter space assures accurate trajectory prediction in DR mode, and offers the consistent positioning performance of less than 2m CEP 50%.

REFERENCES

- [1] Abdel-Hamid, W., Abdelazim, T., El-Sheimy, N., Lachapelle, G., Improvement of MEMS-IMU/GPS performance using fuzzy modeling, GPS Solutions, 10 (2006), 1-11.
- [2] Anderson, R.S., Hanson, D.S., Kourepinis, A.S., Evolution of low cost MEMS/GPS inertial system technologies, International Technical Meeting of the Satellite Division of the ION GPS-2001, September 11-14, 2001, Salt Lake City, Utah, USA, 1332-1343
- [3] Beauregard, S., Haas, H., Pedestrian dead reckoning: a basis for personal positioning, Proceedings of the 3rd Workshop on Positioning, Navigation and Communication, (WPNC'06), March 16, 2006, Hannover, Germany, 27-36.
- [4] Brand, T. J., Phillips, R. E., Foot-to-foot range measurement as an aid to personal navigation, Proceedings of ION 59th Annual Meeting and CIGTF Guidance Test Symposium, June 23-25, 2003, Albuquerque, New Mexico, Alexandria, VA, USA, 113-121.
- [5] Cho, S. Y., Lee, K. W., Lee, J. G., A personal navigation system using low-cost MEMS/GPS/Fluxgate, Proceedings of the ION 59th Annual Meeting, June 23-25 2003, Albuquerque, New Mexico, Alexandria, VA, USA, 122-127.
- [6] Grejner-Brzezinska, D.A., Toth, C. K., Moafipoor, S., Kwon, J., Adaptive knowledge-based system for personal navigation in GPS-denied environments, Proceeding of the ION National Technical Meeting, January 22-24, 2007, San Diego, CA, USA, 517-522.
- [7] Grejner-Brzezinska, D.A., Toth, C. K., Jwa, Y., Moafipoor, S., Kwon, J., Seamless and reliable personal navigator, Proceeding of the ION National Technical Meeting, January 18-20, 2006a, Monterey, California, USA, 597-604.
- [8] Grejner-Brzezinska, D.A., Toth, C. K., Moafipoor, S., Jwa, Y., Kwon, J., Multi-sensor personal navigator supported by human motion dynamics model, Proceeding of the 3rd IAG Symposium on Geodesy for Geotechnical and Structural Engineering, and 12th FIG Symposium on Deformation Measurements, May 22-24, 2006b, Baden, Austria.
- [9] Grejner-Brzezinska, D. A. Wang, J., Gravity modeling for high-accuracy GPS/INS integration, Navigation, 45(3) (1998), 209-220.
- [10] Julier, S. J. Uhlmann, J. K., A new extension of the Kalman filter to nonlinear systems, Proceedings of the SPIE AeroSense, April 20-25, 1997, Orlando, Florida, USA, 182-193.
- [11] Kaygisiz, B. H., Erkmen, A. M., Erkmen, I., GPS/INS enhancement using Neural Networks for autonomous ground vehicle applications, Proceeding of the 2003 IEEE/RSJ (Robotics Society of Japan), October, 2003, Las Vegas, Nevada, USA, Volume 3, 3763-3768.
- [12] Kosko, B., Neural Networks and Fuzzy Systems, 2nd edition, Prentice-Hall, 1991.
- [13] Kourogi, M., Sakata, N., Okuma, T., Kurata, T., Indoor/Outdoor pedestrian navigation with an embedded GPS/RFID/Self-contained sensor system, Proceedings of the 16th International Conference on Artificial Reality and Telexistence (ICAT2006), 2006, 1310-1321.
- [14] Lachapelle, G., Godha, S., Cannon, M.E., Performance of integrated HSGPS-IMU technology for pedestrian navigation under signal masking, Proceeding of European Navigation Conference, Royal Institute of Navigation, ENC-GNSS, May 8-10, 2006, Manchester, U.K, 1-24.
- [15] Liu, J.S., Chen, R., Sequential Monte Carlo Methods for Dynamical System, Journal of the American Statistical Association (ASA), 93 (1998), 1032-1044.
- [16] Principe, J.C., Euliano, N.R., Lefebvre, W.C., Neural and Adaptive Systems, 1st edition, Wiley & Sons, 2000.
- [17] Retscher, G., Thienelt, M., NAVIO-a navigation and guidance service for pedestrians, Journal of Global Positioning Systems (JGPS), 3(1-2) (2004), 208-217.
- [18] Ristic, B., Arulampalam, S., Gordon, N., Beyond the Kalman filter: Particle filters for tracking applications, 1st edition, Artech House, Boston, London, 2004.
- [19] Sasiadek, J.Z., Khe, J., Sensor fusion based on Fuzzy Kalman filter, IEEE Second International Workshop on Robot Motion and Control, October 18-20, 2001, Bukowy Dworek, Poland , 275-283.
- [20] Simon, D., Kalman filtering for fuzzy discrete time dynamic systems, Applied soft computing, 3(3) (2003), 191-207.
- [21] Thienelt, M., Eichhorn, A., Reiterer, A., Roberts, G., Pedestrian positioning without map matching methods - prototype of a knowledge-based Kalman filter, Proceedings of the Joint symposium of Seoul Metropolitan Fora & Second International Workshop on Ubiquitous Pervasive and Internet Mapping, October 23-25, 2006, Seoul, Korea, 148 - 156.
- [22] Wan, E. A., van der Merwe, R., Kalman filtering and Neural Networks, Chap. Chapter.7: The Unscented Kalman Filter, (50 pages), Wiley Publishing, Eds. S. Haykin, 2001.
- [23] Wang, J. J., Wang, J., Sinclair, D., Watts, L., A Neural Network and Kalman filter hybrid approach for GPS/INS integration, 12th IAIN Congress & 2006 International Symposium on GPS/GNSS, Jeju, Korea, October 18-20, 2006, 277-282.
- [24] Yi, Y., Grejner-Brzezinska, D.A., Tightly-coupled GPS/INS integration using unscented Kalman filter and Particle filter, Proceedings of the ION GNSS, September 26-29, 2006a, Fort Worth, Texas, USA, 2182-2191.